

This is an Open Access document downloaded from ORCA, Cardiff University's institutional repository: <https://orca.cardiff.ac.uk/id/eprint/104915/>

This is the author's version of a work that was submitted to / accepted for publication.

Citation for final published version:

Liu, Xijiao, Jiang, Hanyu, Chen, Jie, Zhou, You , Huang, Zixing and Song, Bin 2017. Gadoxetic acid-enhanced MRI outperformed MDCT in diagnosing small hepatocellular carcinoma: A meta-analysis. *Liver Transplantation* 23 (12) , pp. 1505-1518. 10.1002/lt.24867

Publishers page: <http://dx.doi.org/10.1002/lt.24867>

Please note:

Changes made as a result of publishing processes such as copy-editing, formatting and page numbers may not be reflected in this version. For the definitive version of this publication, please refer to the published source. You are advised to consult the publisher's version if you wish to cite this paper.

This version is being made available in accordance with publisher policies. See <http://orca.cf.ac.uk/policies.html> for usage policies. Copyright and moral rights for publications made available in ORCA are retained by the copyright holders.



## Gadoxetic acid-enhanced MRI outperformed MDCT in diagnosing small hepatocellular carcinoma: a meta-analysis

Xijiao Liu<sup>\*,1</sup>, Hanyu Jiang<sup>\*,1</sup>, Jie Chen<sup>\*,1</sup>, You Zhou<sup>2</sup>, Zixing Huang<sup>1</sup>, Bin Song<sup>\*,1</sup>

<sup>1</sup>Department of Radiology, Sichuan University West China Hospital, No. 37 Guoxue Alley, Chengdu, Sichuan Province, China

<sup>2</sup>Systems Immunity Research Institute, Division of Infection and Immunity, School of Medicine, Cardiff University, Cardiff CF14 4XN Wales, United Kingdom

\* These authors contributed equally to this work.

**Keywords:** Gd-EOB-DTPA; magnetic resonance imaging; multidetector computed tomography; HCC; diagnosis

Manuscript ID: LT-17-300

This article has been accepted for publication and undergone full peer review but has not been through the copyediting, typesetting, pagination and proofreading process which may lead to differences between this version and the Version of Record. Please cite this article as an 'Accepted Article', doi: 10.1002/lt.24867

**Abbreviations:**

AUC area under the summary receiver operating characteristic curve

CE-MRI contrast-enhanced magnetic resonance imaging

CI confidence interval

CT computed tomography

DWI diffusion weighted imaging

FN false-negative

FP false-positive

Gd-EOB-DTPA gadoteric acid disodium

HBP hepatobiliary phase

HBV hepatitis B virus

HCV hepatitis C virus

HCC hepatocellular carcinoma

MDCT multidetector computed tomography

QUADAS Quality Assessment of Diagnostic Accuracy Studies

RFA radiofrequency ablation

SROC summary receiver operating characteristic

TACE transcatheter arterial chemoembolization

TN true-negative

TP true-positive

**Funding:** the National Natural Science Foundation 81471658

**No conflicts of interest**

**Corresponding author:** Professor Bin Song. E-mail: songlab\_radiology@163.com. Telephone: +86-28-85423680(O). Fax: +86-28-85423680(O). Address: Department of Radiology, West China Hospital, Sichuan University, Chengdu, Sichuan province, China (postcode: 610041).

**Abstract:**

Early detection of small hepatocellular carcinoma (HCC) lesions can improve long-term patient survival. A systematic review and meta-analysis of the diagnostic performance of gadoxetic acid disodium-enhanced magnetic resonance imaging (Gd-EOB-DTPA-enhanced MRI) and multidetector computed tomography (MDCT) was performed in diagnosing small HCCs measuring up to 2 cm ( $\leq 2$ cm). Two investigators searched multiple databases for studies in which the performances of either Gd-EOB-DTPA-enhanced MRI or MDCT were reported with sufficient data to construct  $2 \times 2$  contingency tables for diagnosing HCCs up to 2 cm on a per-lesion or per-patient level. Diagnostic performances were quantitatively pooled by a bivariate random-effect model with further meta-regression and subgroup analyses. Twenty-seven studies (fourteen on Gd-EOB-DTPA-enhanced MRI, nine on MDCT and four on both) were included, enrolling a total of 1735 patients on Gd-EOB-DTPA-enhanced MRI and 1781 patients on MDCT.

Gd-EOB-DTPA-enhanced MRI demonstrated significantly higher overall sensitivity than did MDCT (0.96 vs 0.65,  $p < 0.01$ ), without substantial loss of specificity (0.98 vs 0.94,  $p > 0.05$ ). Area under the summary receiver operating characteristic curve was 0.9712 with Gd-EOB-DTPA-enhanced MRI and 0.8538 with MDCT. Regarding Gd-EOB-DTPA-enhanced MRI, sensitivity was significantly higher for studies from non-Asian countries than Asian countries (0.96 vs 0.93,  $p < 0.01$ ), for retrospective studies than prospective studies (0.95 vs 0.91,  $p < 0.01$ ), and for those with Gd-EOB-DTPA injection rate  $\geq 1.5$  ml/s than that of  $< 1.5$  ml/s (0.97 vs 0.90,  $p < 0.01$ ). *Conclusions:* Gd-EOB-DTPA-enhanced MRI demonstrated higher sensitivity and overall diagnostic accuracy than MDCT, and thus should be the preferred imaging modality for diagnosing small HCCs measuring up to 2 cm.

## Introduction

Hepatocellular carcinoma (HCC) is the fifth most common cancer, the third leading cause of cancer-related mortality and the most common primary liver malignancies worldwide<sup>1</sup>. It occurs predominantly in patients with liver cirrhosis or chronic liver diseases<sup>2</sup>. Despite advances in treatment options including resection, liver transplantation, local-regional therapy and systematic chemotherapy for HCCs, long-term patient survival still calls for complete curative treatment of the early-stage HCCs, especially lesions smaller than 2 cm<sup>2</sup>.

Currently, non-invasive imaging modalities play significant roles in the characterization and diagnosis of HCCs, with the diagnosis of HCC primarily based on multiphase computed tomography (CT) or contrast-enhanced magnetic resonance imaging (CE-MRI) findings<sup>3,4</sup>. However, small HCCs measuring up to 2 cm in diameter frequently present with atypical imaging features. Therefore, specified as they are, dynamic CT and conventional non-specific contrast-enhanced MRI may not be sensitive enough for small HCC nodules, with sensitivities ranging between 40-56%<sup>5</sup> and 57-75%<sup>6,7</sup>, respectively. Thus, accurate detection and characterization of early HCCs remain one of the most challenging areas in liver imaging.

Fortunately, widespread applications of multidetector CT (MDCT) in recent years have led to improved HCC detection. Moreover, the introduction of a liver-specific hepatobiliary contrast agent-Gadoxetic acid disodium (Gd-EOB-DTPA), has further optimized the diagnostic performances of MRI for liver tumors. Gd-EOB-DTPA-enhanced MRI can provide both the hemodynamic information during early dynamic phases and better lesion characterization regarding hepatocyte presence and function in the hepatobiliary phase (HBP) in a single examination<sup>8</sup>. Several recent studies were dedicated to compare the diagnostic performances between MDCT and Gd-EOB-DTPA-enhanced MRI for small HCCs<sup>9-12</sup>, but their results may have been limited due to small study sample sizes.

Therefore, the aim of our study was to conduct a meta-analysis evaluating and comparing the diagnostic performances of MDCT and Gd-EOB-DTPA-enhanced MRI for characterization of small HCCs measuring up to 2 cm. We also explored factors that may influence the diagnostic accuracies.

## Materials and Methods

**Search Strategy.** Two independent investigators (Xijiao Liu and Hanyu Jiang ) conducted a systematic literature search in Pubmed, Web of Science, EMBASE, Cochrane Library, Springer Link, Science Direct, and Google Scholar to identify relevant articles published before February 10, 2017 with the key words regarding “hepatocellular carcinoma”, “gadolinium ethoxybenzyl DTPA”, “magnetic resonance imaging”, and “multidetector computed tomography”. We restricted our research to articles concerning humans with an abstract in English.

**Study Selection.** The two previously noted investigators independently reviewed the titles, abstracts and full texts of the yielded original articles to determine whether they were eligible for further quantitative analyses. The inclusion criteria were as followed: (1) the article enrolled the diagnostic accuracy of MDCT or Gd-EOB-DTPA for HCC; (2) the article used reference standard based on: a. pathologic proof obtained after liver explant, resection and/or biopsy; b. evidence of conclusive imaging findings comprising arterial hypervascularity and venous or delayed phase washout 3, 4 and/or c. imaging follow-up of at least 6 months; (3) the article constituted an

original research instead of a review article, case report, letter, comment, guideline or a meta-analysis; (4) the study included original data addressing small HCC nodules measuring “up to 2 cm ( $\leq 2$  cm)”, “less than 2 cm ( $< 2$  cm)” or “1-2 cm”; (5) the total study population was more than 20; (6) sufficient data were available to calculate true-positive (TP), false-positive (FP), false-negative (FN) and true-negative (TN) values to construct a  $2 \times 2$  contingency table. Articles were excluded if they were duplicate publications based on the same primary study.

Disagreements between the two reviewers were resolved by consensus. Investigators of the original researches were approached to inquire more information for studies met all of the above criteria apart from sufficient data for the  $2 \times 2$  table.

**Data Extraction and Quality Assessment.** Two investigators (Hanyu Jiang and Jie Chen) reviewed the included studies and extracted the relevant details independently. Any discrepancy between the two investigators was resolved by consensus or consulting a senior radiologist (Bin Song) with more than 20 years of experience in hepatic disease diagnosis.

To extract data of study characteristics, we recorded details regarding study authors, year of publication, country of origin, study design, blinding procedures, patient information, sizes of HCC evaluated, number of HCC lesions within measuring up to 2 cm, determination of results on a per-lesion or per-patient basis, reference standards, et al. We also recorded the image protocols of the following: MR and CT scanner, CT detector rows, CT contrast agents, Gd-EOB-DTPA dosage and injection rate, and inclusion of HBP or diffusion weighted imaging (DWI).

TP, FN, TN, FP data for the performance of MDCT or Gd-EOB-DTPA-enhanced MRI in diagnosing up to 2 cm HCCs of each included study were extracted for the construction of the  $2 \times 2$  contingency table. If any diagnostic accuracy was reported for multiple observers, then the observer with the highest diagnostic accuracy was selected. Moreover, if any diagnostic accuracy was reported according to different imaging criteria, then, as is consistent with the current guidelines<sup>3,4</sup>, the criteria which included both hyper enhancement or wash-in during the arterial phase and hypo enhancement or wash-out during the venous and/or delayed phase were required.

The overall quality and likelihood of bias of the included studies were assessed according to Quality Assessment of Diagnostic Accuracy Studies (QUADAS)<sup>13</sup> by the two previously mentioned investigators (Hanyu Jiang and Jie Chen) independently. Notably, an interval between pathologic examination and the index test of 3 months and above or an overall imaging follow-up of 6 months or less were considered inappropriate. Besides, reference standards based on imaging follow-up of Gd-EOB-DTPA-enhanced MRI or MDCT findings were considered to have overlaps with and include knowledge of the index tests. Publication biases were evaluated with the Deeks funnel plots tests<sup>14</sup>. An inverted symmetrical funnel plot with  $P > 0.05$  was considered to indicate the absence of publication bias<sup>14</sup>. The publication bias was evaluated with Stata software (version 12.0; StataCorp LP, College Station, TX).

**Statistical analysis.** First, the sensitivity, specificity, and the corresponding 95% confidence intervals (CIs) for the diagnosis of small HCCs by MDCT and Gd-EOB-DTPA-enhanced MRI were calculated using a random-effects coefficient binary regression model<sup>15</sup>. We constructed summary receiver operating characteristic (SROC) curves and calculated the corresponding areas under the SROC curve (AUCs) of MDCT and Gd-EOB-DTPA-enhanced MRI to determine the diagnostic performances<sup>16</sup>. All estimations were performed with a multilevel mixed-effects logistic regression module which fitted the bivariate model in Meta-Disc software (version 1.4; Madrid, Spain).

A z test for unpaired groups was performed to compare the sensitivities and specificities of the two modalities with Microsoft Excel 11.0 (Microsoft, Redmond, WA),  $p < 0.05$  was considered to indicate a significant difference.

**Heterogeneity Exploration and Subgroup Analysis.** We evaluated heterogeneity between the included studies for each imaging modality with Meta-Disc software (version 1.4; Madrid, Spain). The heterogeneity was identified by the Q statistic of the Chi-square value test and the inconsistency index ( $I^2$ ), in which  $P < 0.1$  or  $I^2 > 50\%$  indicated presence of heterogeneity<sup>17</sup>. A threshold effect is considered to exist in the presence of a positive correlation between the sensitivity and (1-specificity) of included studies. The absence of threshold effect was confirmed by not noticing the “shoulder-arm” shape in the SROC plane<sup>16</sup>. Upon detection of significant heterogeneity, single-factor meta-regression analyses and subgroup analyses were then performed to determine factors which contributed to the heterogeneity and their quantitative effects on the diagnostic results<sup>18</sup>. The subgroup analyses evaluated factors that could affect diagnostic performance and lead to heterogeneity. Sensitivity and specificity were calculated and compared for pairwise combinations of subgroups of studies defined by each of the recorded study characteristics with Stata software (version 12.0; StataCorp LP, College Station, TX).

## Results

**Study Selection.** 2629 citations were initially identified upon removal of duplicates after the database search, of which 27 studies were in consistent with all the inclusion criteria and included in this meta-analysis<sup>9-12, 19-41</sup> (Fig. 1). Among the included studies, 14 reported test performance of Gd-EOB-DTPA-enhanced MRI<sup>19-32</sup>, 9 of MDCT<sup>33-41</sup>, and 4 of both<sup>9-12</sup>. Different studies reported by the same investigators (Di Martino, M<sup>20, 35, 39</sup>, and Park, MJ<sup>23, 24</sup>.) were included in our final meta-analysis; however, these studies were confirmed not to overlap according to different study periods<sup>23, 24; 35, 39</sup>, or because different imaging modalities were applied<sup>20, 35</sup>.

**Study Characteristics.** Table 1 and Table 2 summarize the important characteristics of the included studies. A total of 1735 patients with 1482 HCC lesions measuring up to 2 cm underwent Gd-EOB-DTPA-enhanced MRI, while a total of 1781 patients with 793 HCC lesions underwent MDCT. Among these, a total of 276 patients underwent the two imaging modalities sequentially<sup>9-12</sup>. Most studies included patients with documented underlying liver cirrhosis or chronic liver disease. Assessment was performed on a per-patient basis in 2 studies<sup>38, 41</sup> with MDCT and a per-lesion basis in the remaining studies. Imaging protocols of the included studies are demonstrated in Supplemental Table 1 and 2.

**Quality Assessment and Publication Biases.** Quality assessment demonstrated that the qualities of the included studies were good. Fig. 2 shows a graphical display of QUADAS results concerning the proportion of included studies for each question. There were overall high scores for most questions from patient selection to explained withdrawals.

The Deeks funnel plot showed that studies were distributed symmetrically on a scatter plot. The p values of the Deeks funnel plot asymmetry test for Gd-EOB-DTPA-enhanced MRI and MDCT were 0.52 and 0.18, respectively, demonstrating no evidence of notable publication bias.

**Diagnostic Performances.** The overall pooled sensitivity of Gd-EOB-DTPA-enhanced MRI was significantly higher than that of MDCT (0.92 [95% CI: 0.90 to 0.93] vs 0.66 [95% CI: 0.63 to 0.70],  $p < 0.01$ ). The overall pooled specificity of Gd-EOB-DTPA-enhanced MRI was slightly lower than that of MDCT, but this difference was not statistically significant (0.89 [95% CI: 0.87

to 0.91] vs 0.91 [95% CI: 0.89 to 0.93],  $p > 0.05$ ). Notably, four studies<sup>9-12</sup> reported diagnostic performances of both Gd-EOB-DTPA-enhanced MRI and MDCT and thus allowed a head-to-head comparison between the two imaging modalities. Similarly, Gd-EOB-DTPA-enhanced MRI demonstrated significantly higher overall sensitivity than MDCT (0.96 [95% CI: 0.93 to 0.99] vs 0.65 [95% CI: 0.57 to 0.73],  $p < 0.01$ ), without substantial loss of specificity (0.94 [95% CI: 0.87 to 1.00] vs 0.98 [95% CI: 0.95 to 1.00],  $p > 0.05$ ). According to the SROC curve, the AUC was 0.9712 with Gd-EOB-DTPA-enhanced MRI and 0.8538 with MDCT. Forest plots of sensitivities and specificities of different imaging modalities are shown in Fig. 3, while the SROC curves in Fig. 4.

**Heterogeneity Assessing and Meta-regression Analysis.** Moderate to substantial heterogeneity was detected in our meta-analysis.  $I^2$  of sensitivity and specificity were 82.0% and 88.7% for Gd-EOB-DTPA-enhanced MRI, while 75.3% and 69.9% for MDCT, respectively. Threshold effects of Gd-EOB-DTPA-enhanced MRI and MDCT were eliminated through the SROC planes, which showed no “shoulder-arm” shapes. Neither single-factor nor multi-factor meta-regression analyses showed any study characteristic that contributed statistically significantly to heterogeneity for Gd-EOB-DTPA-enhanced MRI or MDCT.

**Subgroup Analyses.** As considerable heterogeneity was revealed, we performed subgroup analyses between different study characteristics in Gd-EOB-DTPA-enhanced MRI to evaluate their quantitative effects on heterogeneity (Table. 3). Sensitivities were significantly higher for studies originated from non-Asian countries compared with those originated from Asia (0.96 vs 0.93,  $p < 0.01$ ), those with a retrospective design compared with prospective design (0.95 vs 0.91,  $p < 0.01$ ), and those performed with Gd-EOB-DTPA injection rate  $\geq 1.5$ ml/s compared with  $< 1.5$ ml/s (0.97 vs 0.90,  $p < 0.01$ ), and those performed with sequential Gd-EOB-DTPA-enhanced MRI compared with those not (0.96 vs 0.92,  $p = 0.01$ ). Subgroup analysis was not performed for MDCT due to insufficient studies number (fewer than 4) in each subgroup to perform data-syntheses analysis.

## Discussions

Results of our study showed that Gd-EOB-DTPA-enhanced MRI demonstrated higher sensitivity and overall diagnostic accuracy than MDCT, with AUCs of 0.9712 and 0.8538 respectively. A diagnostic tool is generally defined as perfect if the AUC is 1, excellent if the AUC is greater than 0.9, and good if the AUC is greater than 0.8<sup>42</sup>. According to this, Gd-EOB-DTPA-enhanced MRI had an excellent diagnostic accuracy, while MDCT good for diagnosing small HCCs.

Currently, all major clinical practice guidelines endorse multiphase CT and MR imaging with extracellular contrast agents as the first-line modalities for diagnosis and staging of HCC<sup>3,4</sup>. However, on the basis of our study results, Gd-EOB-DTPA-enhanced MRI should be the preferred modality for evaluating small HCCs because it provided better lesion detection ability and higher overall diagnostic accuracy, without significant loss of specificity.

During hepatocarcinogenesis, most HCCs evolve from histologically abnormal precursor lesions and undergo a multistep from cirrhotic nodules, low-grade dysplastic nodules (LGDNs), high-grade dysplastic nodules (HGDNs), early HCCs to progressed HCCs<sup>43</sup>. During these steps, the intranodular arterial supply decreases initially and increases afterwards<sup>43</sup>. Therefore, despite that progressed HCCs usually show typical arterial hypervascularity compared with background

liver, earlier nodules typically do not. Thus, MDCT and extracellular agents-enhanced MRI demonstrate limited potential in identifying and differentiating early HCCs from the benign liver nodules<sup>5-7</sup> based on typical vascular enhancement patterns. Gd-EOB-DTPA, on the other hand, is taken predominantly by hepatocytes via the organic anion transporter polypeptides OATP1B1/B3 and excreted via the multidrug resistance-associated proteins MRP2<sup>8</sup>. In early HCCs, OATP1B1/B3 expression is usually reduced or absent relative to that of the liver parenchyma, while MRP2 expression is usually elevated<sup>8</sup>. Thus, the accumulation of Gd-EOB-DTPA often diminishes progressively from cirrhotic nodules to progressed HCCs compared to the background liver<sup>8</sup>. In HBP, most HCCs appear as low signal intensity foci against the enhancing high signal parenchyma in the HBP. This nature enables Gd-EOB-DTPA-enhanced MRI to be highly sensitive for the diagnosis of early HCC lesions and for their differentiation from DNs and vascular pseudolesions, in which the delayed hypointensity in HBP is often absent<sup>10</sup>.

Our research revealed that Gd-EOB-DTPA-enhanced MRI demonstrated a significantly higher sensitivity and overall accuracy for small HCCs than multiphase MDCT without substantial loss of specificity, which was in accordance with several previous comparative studies. Onishi et al<sup>44</sup> retrospectively analyzed 73 hypervascular HCC lesions from 31 suspected HCC patients, and found that for the subgroup with lesions less than 1 cm the combined dynamic and HBP MR images with Gd-EOB-DTPA demonstrated a significantly higher sensitivity than MDCT (48% vs 11%,  $p < 0.001$ ); while with lesions 1–2 cm the mean sensitivity for combined MRI was higher than multiphase MDCT (75% vs 58%) as well, although the difference was not statistically significant. Likewise, Tsurusaki et al<sup>45</sup> included fifty-four patients with 83 histopathologically confirmed HCCs in their study. They reported that the combined interpretation of the dynamic and HBP of Gd-EOB-DTPA-enhanced MRI showed statistically higher sensitivity for lesion detection than multiphase MDCT images in the nineteen  $\leq 1$  cm lesions (58% vs 28%,  $p = 0.0037$ ) and thirty-two 1-2 cm lesions (84% vs 73%,  $p = 0.015$ ). Böttcher et al<sup>46</sup> also retrospectively analyzed 29 patients with 130 liver lesions and revealed that for HCC lesions  $< 20$  mm, Gd-EOB-DTPA-enhanced MRI was able to detect more lesions, with 10.3% and 23.7% of lesions missed by MRI and MDCT respectively, and yielded a significantly higher diagnostic accuracy than MDCT (88.9% vs 67.6%,  $p < 0.01$ ).

A possible explanation is that, as discussed above, functional changes of OATP1B1/B3 and MRP2 usually happen ahead of neovascularization and are more specific hallmarks for early HCCs during hepatocarcinogenesis. Therefore, since diagnosis of HCC with MDCT is predominantly dependent on the typical vascular patterns, Gd-EOB-DTPA-enhanced MRI is able to identify the minute HCC lesions at an earlier stage.

Nevertheless, this finding can also be the result that, more retrospective studies were included on Gd-EOB-DTPA-enhanced MRI than did MDCT (13/18 retrospective studies of Gd-EOB-DTPA-enhanced MRI vs 4/13 retrospective studies of MDCT) in our study. As retrospective studies are more likely to cause a bias toward increased diagnostic sensitivity<sup>47</sup>, this may have resulted in overestimated sensitivity of Gd-EOB-DTPA-enhanced MRI for diagnosing small HCCs. Besides, it should be recognized that Gd-EOB-DTPA-enhanced MRI is more expensive, less available, less rapid, less robust, more sensitive to motion artifact and require more expertise to perform and interpret images compared with MDCT. Therefore, Gd-EOB-DTPA-enhanced MRI may not be recommended in communities or less-specialized medical centers, and that more researches are needed to optimize the timing and image quality of

Gd-EOB-DTPA-enhanced MRI for characterizing small HCCs precisely.

The subgroup analysis revealed that Gd-EOB-DTPA injection rate  $\geq 1.5$  ml/s was associated significantly with increased sensitivity (0.97 vs 0.90,  $p < 0.01$ ) for small HCCs without loss of specificity (0.92 vs 0.95,  $p = 0.34$ ). However, this was not in line with previous studies. Currently, some believe that lower injection rates of Gd-EOB-DTPA are more likely to lead to higher relaxivity that can help avoid saturation effect and thus result in increased probability of obtaining optimal hepatic arterial phase timing with the help of better arterial enhancement and decreased patients' discomfort<sup>48</sup>. Chung et al<sup>48</sup> revealed that, with their study performed on a 3.0-T MR system, gadoteric acid injection rates of 1 ml/s rate and 2 ml/s ensured comparable image quality and detection of focal hypervascular hepatic lesions, but nearly half of their included HCC lesions were  $> 2$  cm (11/24 of 1 ml/s and 10/21 of 2 ml/s). On the other hand, another study showed that 1 ml/s injection rate achieved greater aorta enhancement and aortic perfusion parameters than 2 ml/s on a 1.5-T MR system<sup>49</sup>. However, the included patients were not restricted to have HCCs, and diagnostic performances were not evaluated in their study neither. The difference between our result and these studies may have been due to different lesion size ranges, experience of radiologists and image quality among medical centers. Therefore, further prospective studies in consecutive patients are needed to refine and validate the best injection rate of Gd-EOB-DTPA for diagnosing small HCCs.

The subgroup analysis also showed that, for Gd-EOB-DTPA-enhanced MRI, retrospective studies demonstrated higher sensitivity than did prospective studies (0.95 vs 0.91,  $p < 0.01$ ), of which the possible explanation has been discussed above.

Another interesting result of the subgroup analysis was that studies originated from non-Asian (Italy and USA) countries demonstrated significantly higher sensitivity than did studies from Asian countries (0.96 vs 0.93,  $p = 0.01$ ). This could be explained by earlier introduction of Gd-EOB-DTPA-enhanced MRI in Italy and USA, resulting in increased experience of radiologists in diagnosing small HCCs. However, this finding was not in keep with previous studies. Kierans et al<sup>6</sup> conducted a meta-analysis on the diagnostic performance of MRI for  $\leq 2$  cm HCCs with 22 studies, their result revealed that Asian studies yielded higher sensitivity than other studies, but this difference was eliminated after adjusting for the effect of inclusion of HBP. Nevertheless, their result was based on all MRI modalities without excluding contrast agents except for Gd-EOB-DTPA. Besides, while our research involved 18 studies considering Gd-EOB-DTPA, Kierans et al only included 7.

Our meta-analysis has several limitations. First, we included limited number of prospective studies in our research. This may have led to a major methodologic limitation of collecting and pooling many suboptimal retrospective data, resulting in overestimated diagnostic sensitivity. Second, only studies published in English were included in our meta-analysis, possibly to have led to the "Tower of Babel" bias in which the non-English speaking authors tend to only submit studies with positive results to international journals published in English<sup>50</sup>.

Third, substantial heterogeneity was detected for both Gd-EOB-DTPA-enhanced MRI and MDCT, which may have affected the general applicability of the summary estimates. Therefore, we implied the summary ROC model and the random effects model to overcome the heterogeneity of our data. With relatively narrow 95% CI, we believe that our results should be valuable in clinical practices. Moreover, single-factor meta-regression analyses and subgroup analyses were conducted to determine factors which contributed to the heterogeneity and their quantitative

effects on the diagnostic results. However, several sources of heterogeneity including patient disease severity, radiologists' experience difference and pathologists' criteria variation, may not have been well explored in our meta-analysis, so the heterogeneity remained a point of concern. Fourth, we didn't conduct a subgroup analysis for MDCT due to limited number of studies for each study characteristic.

Finally, only four included studies<sup>9-12</sup> evaluating the diagnostic performances of both Gd-EOB-DTPA and MDCT for small HCCs were available and included. In these studies, a total of 276 patients underwent the two imaging modalities sequentially, allowing the most reliable head-to-head comparison. However, the quality of quantitative analysis might have been affected by the limited number of studies. In order to deal with this issue, an unpaired comparison involving all of the included studies was established. As revealed by the pooled results, Gd-EOB-DTPA-enhanced MRI demonstrated significantly higher sensitivities than MDCT in either head-to-head or unpaired comparisons, without substantial loss of specificities. These findings indicated that our unpaired data were reliable. But this methodology may have introduced biases which couldn't be resolved yet. Therefore, more large-scale, prospective studies assessing the test performances of both Gd-EOB-DTPA and MDCT based on same cohorts are encouraged.

In conclusion, Gd-EOB-DTPA-enhanced MRI, compared with multiphasic MDCT, demonstrated better sensitivity and overall accuracy without loss of specificity, especially with higher injection rate of  $\geq 1.5$  ml/s. Therefore, Gd-EOB-DTPA-enhanced MRI should be the preferred imaging modality for the diagnosis of small HCCs measuring up to 2cm.

#### References:

1. Torre LA, Bray F, Siegel RL, Ferlay J, Lortet-Tieulent J, Jemal A. Global cancer statistics, 2012. *CA Cancer J Clin* 2015; 65(2): 87-108.
2. Forner A, Llovet JM, Bruix J. Hepatocellular carcinoma. *Lancet* 2012; 379(9822):1245-1255.
3. Bruix J, Sherman M. American Association for the Study of Liver Diseases. Management of hepatocellular carcinoma: an update. *Hepatology* 2011; 53(3):1020-1022.
4. European Association for Study of Liver; European Organisation for Research and Treatment of Cancer. EASL-EORTC clinical practice guidelines: management of hepatocellular carcinoma. *J Hepatol* 2012; 48(5): 599-641.
5. Lee YJ, Lee JM, Lee JS, Lee HY, Park BH, Kim YH, et al. Hepatocellular carcinoma: diagnostic performance of multidetector CT and MR imaging—a systematic review and meta-analysis. *Radiology* 2015; 275(1): 97-109.
6. Kierans AS, Kang SK, Rosenkrantz AB. The Diagnostic Performance of Dynamic Contrast-enhanced MR Imaging for Detection of Small Hepatocellular Carcinoma Measuring Up to 2 cm: A Meta-Analysis. *Radiology* 2016; 278(1): 82-94.
7. Rimola J, Forner A, Tremosini S, Reig M, Vilana R, Bianchi L, et al. Non-invasive diagnosis of hepatocellular carcinoma  $\leq 2$  cm in cirrhosis. Diagnostic accuracy assessing fat, capsule and signal intensity at dynamic MRI. *J Hepatol* 2012; 56(6):1317-1323.
8. Van Beers BE, Pastor CM, Hussain HK. Primovist, Eovist: what to expect? *J Hepatol* 2012; 57(2):421-429.
9. Sun HY, Lee JM, Shin CI, Lee DH, Moon SK, Kim KW, et al. Gadoxetic acid-enhanced magnetic resonance imaging for differentiating small hepatocellular carcinomas ( $<$  or  $=$  2 cm in diameter) from arterial enhancing pseudolesions: special emphasis on hepatobiliary phase

- imaging. *Invest Radiol* 2010;45(2):96-103.
10. Sano K, Ichikawa T, Motosugi U, Sou H, Muhi AM, et al. Imaging study of early hepatocellular carcinoma: usefulness of gadoxetic acid-enhanced MR imaging. *Radiology* 2011; 261(3):834-844.
  11. Granito A, Galassi M, Piscaglia F, Romanini L, Lucidi V, Renzulli M, et al. Impact of gadoxetic acid (Gd-EOB-DTPA)-enhanced magnetic resonance on the non-invasive diagnosis of small hepatocellular carcinoma: a prospective study. *Aliment Pharmacol Ther* 2013; 37(3):355-363.
  12. Chen N, Motosugi U, Morisaka H, Ichikawa S, Sano K, Ichikawa T, et al. Added Value of a Gadoxetic Acid-enhanced Hepatocyte-phase Image to the LI-RADS System for Diagnosing Hepatocellular Carcinoma. *Magn Reson Med Sci* 2016; 15(1):49-59.
  13. Whiting P, Rutjes AW, Reitsma JB, Bossuyt PM, Kleijnen J. The development of QUADAS: a tool for the quality assessment of studies of diagnostic accuracy included in systematic reviews. *BMC Med Res Methodol* 2003; 3:25.
  14. Sterne JA, Sutton AJ, Ioannidis JP, Terrin N, Jones DR, Lau J, et al. Recommendations for examining and interpreting funnel plot asymmetry in meta-analyses of randomised controlled trials. *BMJ* 2011; 343: d4002.
  15. Reitsma JB, Glas AS, Rutjes AW, Scholten RJ, Bossuyt PM, Zwinderman AH. Bivariate tomoganalysis of sensitivity and specificity produces informative summary measures in diagnostic reviews. *J Clin Epidemiol* 2005; 58(10): 982-990.
  16. Arends LR, Hamza TH, van Houwelingen JC, Heijnenbrok-Kal MH, HuninkMG, Stijnen T. Bivariate random effects meta-analysis of ROC curves. *Med Decis Making* 2008; 28(5): 621-638.
  17. Higgins JP, Thompson SG. Quantifying heterogeneity in a meta-analysis. *Stat Med* 2002; 21(11): 1539-1558.
  18. Dinnes J, Deeks J, Kirby J, Roderick P. A methodological review of how heterogeneity has been examined in systematic reviews of diagnostic test accuracy. *Health Technol Assess* 2005; 9(12): 1-113.
  19. Ahn SS, Kim MJ, Lim JS, Hong HS, Chung YE, Choi JY. Added value of gadoxetic acid-enhanced hepatobiliary phase MR imaging in the diagnosis of hepatocellular carcinoma. *Radiology* 2010; 255(2): 459-466.
  20. Di Martino M, Marin D, Guerrisi A, Baski M, Galati F, Rossi M, et al. Intraindividual comparison of gadoxetate disodium-enhanced MR imaging and 64-section multidetector CT in the Detection of hepatocellular carcinoma in patients with cirrhosis. *Radiology* 2010; 256(3): 806-816.
  21. Golfieri R, Renzulli M, Lucidi V, Corcioni B, Trevisani F, Bolondi L. Contribution of the hepatobiliary phase of Gd-EOB-DTPA-enhanced MRI to Dynamic MRI in the detection of hypovascular small ( $\leq 2$  cm) HCC in cirrhosis. *Eur Radiol* 2011; 21(6): 1233-1242.
  22. Kim YK, Kim CS, Han YM, Yu HC, Choi D. Detection of small hepatocellular carcinoma: intraindividual comparison of gadoxetic acid-enhanced MRI at 3.0 and 1.5 T. *Invest Radiol* 2011; 46(6): 383-389.
  23. Park MJ, Kim YK, Lee MW, Lee WJ, Kim YS, Kim SH, et al. Small hepatocellular carcinomas: improved sensitivity by combining gadoxetic acid-enhanced and diffusion-weighted MR imaging patterns. *Radiology* 2012; 264(3): 761-770.

24. Park MJ, Kim YK, Lee MH, Lee JH. Validation of diagnostic criteria using gadoxetic acid-enhanced and diffusion-weighted MR imaging for small hepatocellular carcinoma ( $\leq 2.0$  cm) in patients with hepatitis-induced liver cirrhosis. *Acta Radiol* 2013; 54(2): 127-136.
25. Hwang J, Kim YK, Kim JM, Lee WJ, Choi D, Hong SS. Pretransplant diagnosis of hepatocellular carcinoma by gadoxetic acid-enhanced and diffusion-weighted magnetic resonance imaging. *Liver Transpl* 2014; 20(12): 1436-1446.
26. Zhao XT, Li WX, Chai WM, Chen KM. Detection of small hepatocellular carcinoma using gadoxetic acid-enhanced MRI: Is the addition of diffusion-weighted MRI at 3.0T beneficial? *J Dig Dis* 2014; 15(3): 137-145.
27. Faletti R, Cassinis MC, Fonio P, Bergamasco L, Pavan LJ, Rapellino A, et al. Multiparametric Gd-EOB-DTPA magnetic resonance in diagnosis of HCC: dynamic study, hepatobiliary phase, and diffusion-weighted imaging compared to histology after orthotopic liver transplantation. *Abdom Imaging* 2015; 40(1): 46-55.
28. Joo I, Lee JM, Lee DH, Jeon JH, Han JK, Choi BI. Noninvasive diagnosis of hepatocellular carcinoma on gadoxetic acid-enhanced MRI: can hypointensity on the hepatobiliary phase be used as an alternative to washout? *Eur Radiol* 2015; 25(10): 2859-2868.
29. Kwon HJ, Byun JH, Kim JY, Hong GS, Won HJ, Shin YM, et al. Differentiation of small ( $\leq 2$  cm) hepatocellular carcinomas from small benign nodules in cirrhotic liver on gadoxetic acid-enhanced and diffusion-weighted magnetic resonance images. *Abdom Imaging* 2015; 40(1): 64-75.
30. Pahade JK, Juice D, Staib L, Israel G, Cornfeld D, Mitchell K, Weinreb J. Is there an added value of a hepatobiliary phase with gadoxetate disodium following conventional MRI with an extracellular gadolinium agent in a single imaging session for detection of primary hepatic malignancies? *Abdom Radiol* 2016; 41(7): 1270-1284.
31. Yim SY, Park BJ, Um SH, Han NY, Sung DJ, Cho SB, et al. Diagnostic performance of gadoxetic acid (Primovist)-enhanced MR imaging versus CT during hepatic arteriography and portography for small hypervascular hepatocellular carcinoma. *Medicine (Baltimore)* 2016; 95(39): e4903.
32. Choi SH, Byun JH, Lim YS, Yu E, Lee SJ, Kim SY, et al. Diagnostic criteria for hepatocellular carcinoma  $\leq 3$  cm with hepatocyte-specific contrast-enhanced magnetic resonance imaging. *J Hepatol* 2016; 64(5): 1099-1107.
33. Bolondi L, Gaiani S, Celli N, Golfieri R, Grigioni WF, Leoni S, et al. Characterization of small nodules in cirrhosis by assessment of vascularity: the problem of hypovascular hepatocellular carcinoma. *Hepatology* 2005; 42(1): 27-34.
34. Ichikawa T, Nakajima H, Nanbu A, Hori M, Araki T. Effect of injection rate of contrast material on CT of hepatocellular carcinoma. *AJR Am J Roentgenol* 2006; 186(5): 1413-1418.
35. Di Martino M, Marin D, Guerrisi A, Baski M, Galati F, Rossi M, et al. Intraindividual comparison of gadoxetate disodium-enhanced MR imaging and 64-section multidetector CT in the Detection of hepatocellular carcinoma in patients with cirrhosis. *Radiology* 2010; 256(3): 806-816.
36. Sangiovanni A, Manini MA, Iavarone M, Romeo R, Forzenigo LV, Fraquelli M, et al. The diagnostic and economic impact of contrast imaging techniques in the diagnosis of small hepatocellular carcinoma in cirrhosis. *Gut* 2010; 59(5): 638-644.
37. Khalili K, Kim TK, Jang HJ, Haider MA, Khan L, Guindi M, Sherman M. Optimization of

- imaging diagnosis of 1-2 cm hepatocellular carcinoma: an analysis of diagnostic performance and resource utilization. *J Hepatol* 2011; 54(4): 723-728.
38. Sersté T, Barrau V, Ozenne V, Vullierme MP, Bedossa P, Farges O, et al. Accuracy and disagreement of computed tomography and magnetic resonance imaging for the diagnosis of small hepatocellular carcinoma and dysplastic nodules: role of biopsy. *Hepatology* 2012; 55(3): 800-806.
  39. Di Martino M, De Filippis G, De Santis A, Geiger D, Del Monte M, Lombardo CV, et al. Hepatocellular carcinoma in cirrhotic patients: prospective comparison of US, CT and MR imaging. *Eur Radiol* 2013; 23(4): 887-896.
  40. Jang HJ, Kim TK, Khalili K, Yazdi L, Menezes R, Park SH, Sherman M. Characterization of 1-to 2-cm liver nodules detected on hcc surveillance ultrasound according to the criteria of the American Association for the Study of Liver Disease: is quadruphase CT necessary? *AJR Am J Roentgenol* 2013; 201(2): 314-321.
  41. Lin MT, Wang CC, Cheng YF, Eng HL, Yen YH, Tsai MC, Tseng PL. Comprehensive Comparison of Multiple-Detector Computed Tomography and Dynamic Magnetic Resonance Imaging in the Diagnosis of Hepatocellular Carcinoma with Varying Degrees of Fibrosis. *PLoS One* 2016; 11(11): e0166157.
  42. Swets JA. Measuring the accuracy of diagnostic systems. *Science* 1988; 240(4857): 1285-1293.
  43. Choi JY, Lee JM, Sirlin CB. CT and MR imaging diagnosis and staging of hepatocellular carcinoma: part I. Development, growth, and spread: key pathologic and imaging aspects. *Radiology* 2014; 272(3): 635-654.
  44. Onishi H, Kim T, Imai Y, Hori M, Nagano H, Nakaya Y, et al. Hypervascular hepatocellular carcinomas: detection with gadoxetate disodium-enhanced MR imaging and multiphase multidetector CT. *Eur Radiol* 2012; 22(4): 845-854.
  45. Tsurusaki M, Sofue K, Isoda H, Okada M, Kitajima K, Murakami T. Comparison of gadoxetic acid-enhanced magnetic resonance imaging and contrast-enhanced computed tomography with histopathological examinations for the identification of hepatocellular carcinoma: a multicenter phase III study. *J Gastroenterol* 2016; 51(1):71-79.
  46. Böttcher J, Hansch A, Pfeil A, Schmidt P, Malich A, Schneeweiss A, et al. Detection and classification of different liver lesions: comparison of Gd-EOB-DTPA-enhanced MRI versus multiphase spiral CT in a clinical single centre investigation. *Eur J Radiol* 2013; 82(11): 1860-1869.
  47. Deeks J. Systematic reviews of evaluations of diagnostic and screening tests. In: Egger M, Smith GD, Altman DG, eds. *Systematic reviews in health care: meta-analysis in context*. 2nd ed. London, England: BMJ Books 2001; 248-282.
  48. Chung SH, Kim MJ, Choi JY, Hong HS. Comparison of two different injection rates of gadoxetic acid for arterial phase MRI of the liver. *J Magn Reson Imaging* 2010; 31(2): 365-372.
  49. Schmid-Tannwald C, Herrmann K, Oto A, Panteleon A, Reiser M, Zech C. Optimization of the dynamic, Gd-EOB-DTPA-enhanced MRI of the liver: the effect of the injection rate. *Acta Radiol* 2012; 53(9): 961-965.
  50. Grégoire G, Derderian F, Le Lorier J. Selecting the language of the publications included in a meta-analysis: is there a Tower of Babel bias? *J Clin Epidemiol* 1995; 48(1): 159-163.

**Table 1. Characteristics of the included 18 MRI studies**

No	Study	Year published	Nationality	T	F	T	F	No. of Patients	No. of HCC Lesions	HCC Size	Study Design	Enrollment patients	Reference Standard
1	Anh <sup>19</sup>	2010	Korea	25	0	3	1	59	26	1-2cm	Retro	consecutive cirrhosis patients, 12mo(4/07-3/08)	Surgical findings, biopsy, lipiodol uptake after TACE, or imaging follow-up
2	Di Martino <sup>20</sup>	2010	Italy	47	2	18	8	58	55	≤2cm	pro	consecutive cirrhosis patients, 21mo(2/07-10/08)	Pathologic proof, conclusive imaging result, or imaging follow-up
3	Sun <sup>9</sup>	2010	Korea	31	2	25	2	69	44	≤2cm	Retro	consecutive cirrhosis patients, 10mo(5/08-2/09)	Biopsy, resection, angiography, lipiodol uptake after TACE, or serum a-fetoprotein level
4	Golfieri <sup>21</sup>	2011	Italy	17	2	40	1	127	173	≤2cm	Pro	consecutive cirrhosis patients, 18mo(5/08-10/09)	Surgical findings, biopsy, lipiodol uptake after TACE, or imaging follow-up
5	Kim <sup>22</sup>	2011	Korea	50	0	3	4	40	54	≤2cm	Pro	consecutive patients, 11mo(8/09-6/10)	Surgical findings, characteristic imaging results, lipiodol uptake after TACE, or imaging follow-up
6	Sano <sup>10</sup>	2011	Japan	88	6	155	3	64	96	≤2cm	Retro	consecutive patients, 23mo(1/08-11/09)	Surgical findings and Pathologic proof
7	Park <sup>23</sup>	2012	Korea	16	3	141	13	130	179	≤2cm	Retro	consecutive patients, 15mo(5/09-7/10)	Surgical findings and Pathologic proof, biopsy
8	Park <sup>24</sup>	2013	Korea	10	3	20	1	108	102	≤2cm	Retro	consecutive cirrhosis patients, 17mo(4/10-8/11)	Surgical findings and Pathologic proof, biopsy
9	Granito <sup>11</sup>	2013	Italy	24	3	5	0	33	24	1-2cm	Pro	consecutive cirrhosis patients, 59mo(12/08-10/13)	Biopsy and imaging follow up )
10	Hwang <sup>25</sup>	2014	Korea	47	3	43	21	63	68	≤2cm	Retro	consecutive patients, 67mo(4/08-10/13)	Surgical findings and Pathologic proof
11	Zhao <sup>26</sup>	2014	China	33	4	16	1	33	34	≤2cm	Retro	consecutive cirrhosis patients, 17mo(8/11-12/12)	Pathologic proof, conclusive imaging result, or lipiodol uptake after TACE
12	Faletti <sup>27</sup>	2015	Italy	27	0	10	2	28	28	<2cm	Retro	consecutive cirrhosis patients, 34mo(1/10-10/12)	Surgical findings and Pathologic proof
13	Joo <sup>28</sup>	2015	Korea	78	6	64	19	288	97	<2cm	Retro	consecutive patients, 9mo(9/12-5/13)	Pathologic proof, conclusive imaging result, or imaging follow-up
14	Kwon <sup>29</sup>	2015	Korea	20	9	52	21	230	222	≤2cm	Retro	consecutive cirrhosis	Surgical findings and

				1								patients,20mo(11/09-6/11)	Pathologic proof, biopsy
15	Chen <sup>12</sup>	2016	Japan	41	1	22	2	139	43	<2cm	Retro	consecutive patients,70mo(1/08-10/13)	Surgical findings and Pathologic proof, biopsy
16	Pahade <sup>30</sup>	2016	American	9	11	12	1	30	12	≤2cm	Retro	consecutive patients,30mo(1/10-6/12)	Surgical findings and Pathologic proof, biopsy
17	Yim <sup>31</sup>	2016	Korea	31	0	81	3	38	131	≤2cm	Retro	consecutive cirrhosis patients,36mo(1/08-12/10)	Pathologic proof, conclusive imaging result, or imaging follow-up
18	Choi <sup>32</sup>	2016	Korea	78	21	69	16	198	94	≤2cm	Pro	consecutive cirrhosis patients,12mo(1/11-12/11)	Pathologic proof, marginal recurrence after TACE or RFA, or imaging follow-up
<p>TP, true-positive; FP, false-positive; TN, true-negative;FN, false-negative; †, the number of HCC lesions of the corresponding sizes; TACE transcatheter arterial chemoembolization; RFA radiofrequency ablation.</p>													

**Table 2. Characteristics of the included 13 MDCT studies**

No	Study	Year published	Nation	T P	F P	T N	F N	No. of Patients	No. of HCC Lesions†	HCC Size	Study Design	Enrollment patients	Reference Standard
1	Bolondi <sup>33</sup>	2005	Italy	9	1	11	10	59	29	1-2cm	Pro	consecutive cirrhosis patients,18mo(10/02-3/04)	Biopsy,conclusive imaging result, or imaging follow-up
2	Ichikawa <sup>34</sup>	2005	Japan	36	38	227	5	60	76	<2cm	Pro	consecutive cirrhosis patients,26mo(8/00-9/02)	Biopsy,conclusive imaging result, or imaging follow-up
3	Di Martino <sup>35</sup>	2010	Italy	33	3	17	22	58	55	≤2cm	Pro	consecutive cirrhosis patients,21mo(2/07-10/08)	Pathologic proof,conclusive imaging result, or imaging follow-up
4	Sangiiovanni <sup>36</sup>	2010	Italy	15	0	21	19	64	34	1-2cm	Pro	consecutive cirrhosis patients	Biopsy
5	Sun <sup>9</sup>	2010	Korea	18	1	26	15	69	44	≤2cm	Retro	consecutive cirrhosis patients,9mo(5/08-1/09)	Biopsy, resection, angiography, lipiodol uptake after TACE, or serum a-fetoprotein level
6	Khalili <sup>37</sup>	2011	Canada	18	6	61	16	84	101	1-2cm	Pro	consecutive cirrhosis patients	Pathologic proof, or imaging follow-up
7	Sano <sup>10</sup>	2011	Japan	62	4	157	29	64	96	≤2cm	Retro	consecutive patients,23mo(1/08-11/09)	Resection and Pathologic proof
8	Serste <sup>38</sup>	2012	France	35	5	22	12	74	47	1-2cm	Pro	consecutive patients,60mo(1/05-12/10)	Biopsy
9	Di Martino <sup>39</sup>	2013	Italy	54	5	42	29	140	105	≤2cm	Pro	consecutive cirrhosis patients,43mo(1/07-7/10)	Pathologic proof, or imaging follow-up
10	Granito <sup>11</sup>	2013	Italy	12	0	8	12	33	24	1-2cm	Pro	consecutive cirrhosis patients,38mo(12/08-1/11)	Biopsy and imaging follow up
11	Jang <sup>40</sup>	2013	Korea	21	3	71	15	96	36	1-2cm	pro	consecutive patients,32mo(1/06-8/08)	Pathologic proof, recurrence or metastasis after local ablation therapy, or imaging follow-up
12	Chen <sup>12</sup>	2016	Japan	32	0	23	11	139	43	<2cm	Retro	consecutive patients,70mo(1/08-10/13)	Surgical findings and Pathologic proof and biopsy
13	Lin <sup>41</sup>	2016	China	84	8	20	19	841	103	1-2cm	Retro	consecutive patients,58mo(1/06-10/10)	Surgical findings and Pathologic proof

TP, true-positive; FP, false-positive; TN, true-negative;FN, false-negative; †, the number of HCC lesions of the corresponding sizes; TACE transcatheter arterial chemoembolization.

**Table 3. Subgroup analysis**

Subgroup	No. of Studies	Pooled Sensitivity (95% CI)	P value	Pooled Specificity (95% CI)	P value
<b>Country</b>					
Asian	13	0.93(0.89-0.97)	<0.01	0.94(0.90-0.98)	>0.99
Others	5	0.96(0.92-0.99)		0.85(0.72-0.99)	
<b>Design</b>					
Prospective	5	0.91(0.83-0.98)	<0.01	0.88(0.77-0.99)	0.05
Retrospective	13	0.95(0.91-0.98)		0.94(0.89-0.98)	
<b>Cirrhosis</b>					
With cirrhosis	12	0.94(0.90-0.98)	0.08	0.93(0.89-0.98)	0.54
Without cirrhosis	6	0.93(0.87-0.99)		0.89(0.79-0.99)	
<b>Field Strength</b>					
1.5T	8	0.93(0.88-0.99)	0.06	0.92(0.86-0.99)	0.18
3.0T	6	0.95(0.91-0.99)		0.94(0.89-0.99)	
<b>Gd-EOB-DTPA injection rate</b>					
<1.5ml/s	10	0.90(0.85-0.95)	<0.01	0.95(0.91-0.99)	0.34
≥1.5ml/s	6	0.97(0.95-0.99)		0.92(0.85-0.99)	
<b>HBP</b>					
With HBP	18	0.94(0.91-0.97)	0.35	0.91(0.86-0.96)	0.15
Without HBP	4	0.88(0.78-0.98)		0.96(0.90-0.99)	
<b>Lesion Diameter</b>					
<2cm	18	0.94(0.91-0.97)	0.89	0.92(0.88-0.97)	0.19
<1cm	6	0.83(0.70-0.97)		0.93(0.86-0.99)	
<b>Sequential test</b>					
Yes	4	0.96(0.93-0.99)	0.01	0.94(0.87-1.00)	0.36
No	14	0.92(0.88-0.96)		0.92(0.88-0.96)	

Gd-EOB-DTPA, gadoxetic acid disodium; HBP, hepato-biliary phase.

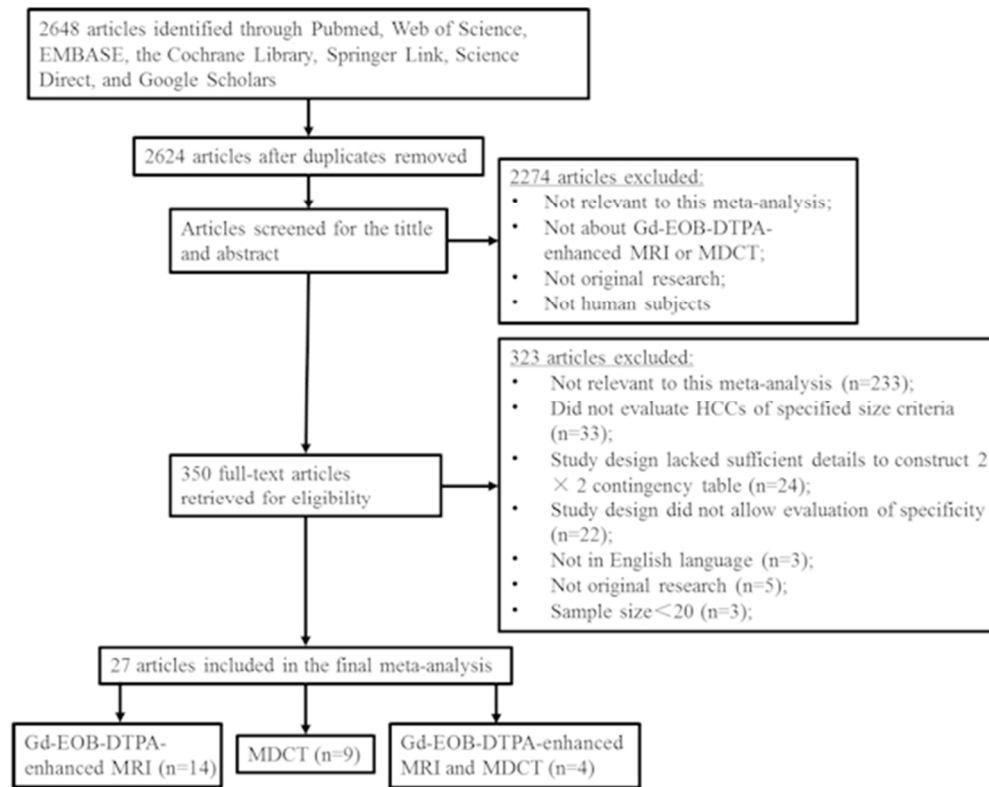


Fig.1 Flowchart illustrating the selection of studies

52x41mm (300 x 300 DPI)

Accep

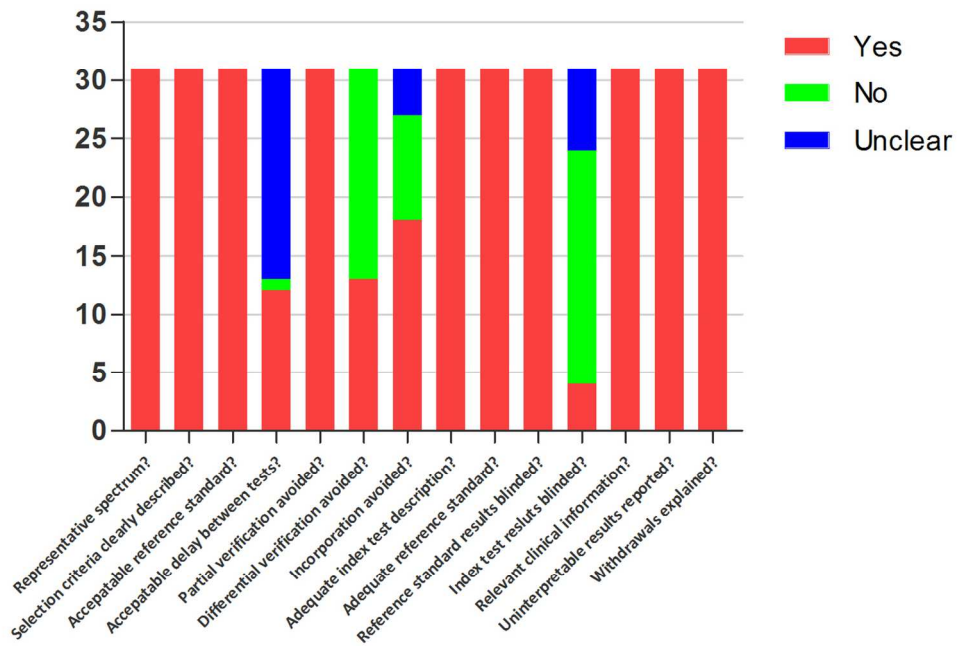


Fig.2 Methodological quality of the 31 included studies

123x87mm (300 x 300 DPI)

Accept

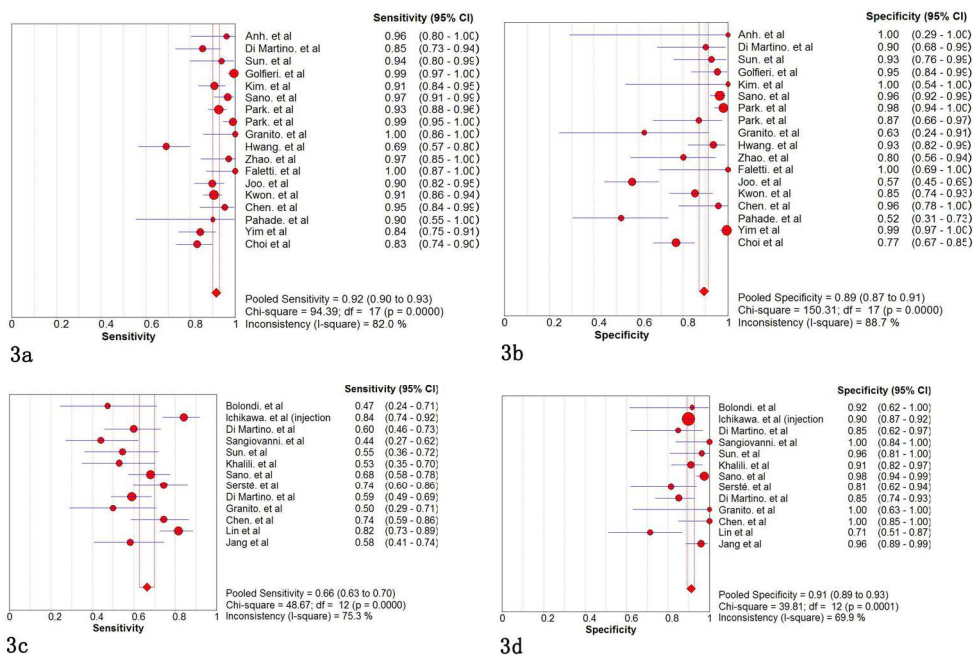


Fig.3 Forest plots of sensitivities and specificities of gadoteric acid disodium-enhanced magnetic resonance imaging(3a,3b) and multidetector computed tomography(3c,3d) for small HCC

169x116mm (300 x 300 DPI)

Accept

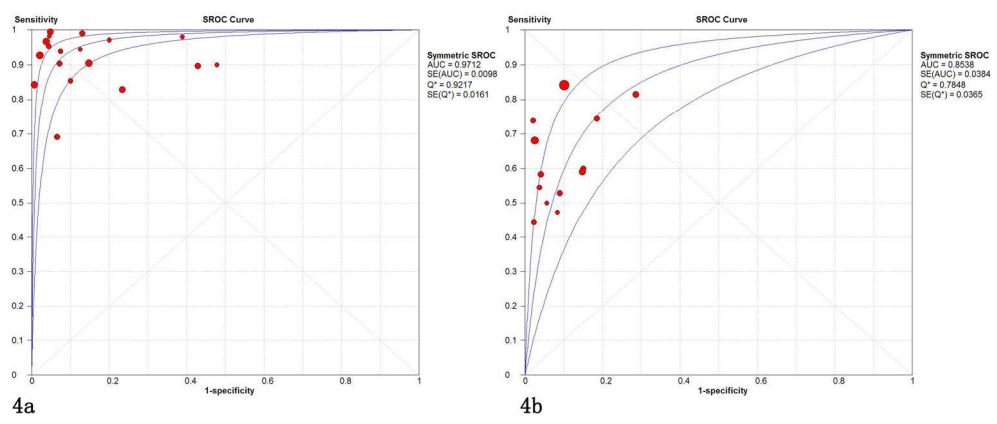


Fig.4 Summary receiver operating characteristic (SROC) curves of gadoxetic acid disodium-enhanced magnetic resonance imaging (4a) and multidetector computed tomography (4b) for small HCCs measuring up to 2 cm( $\leq 2$ cm)

169x70mm (300 x 300 DPI)

Accepted